

Hepatitis C Virus NS3 Protease and Helicase Inhibitors from Red Sea Sponge (*Amphimedon*) Species in Green Synthesized Silver Nanoparticles Assisted by in Silico Modeling and Metabolic Profiling

This article was published in the following Dove Press journal:
International Journal of Nanomedicine

Nourhan Hisham Shady¹
Amira R Khattab²
Safwat Ahmed³
Miaomiao Liu⁴
Ronald J Quinn⁵
Mostafa A Fouad⁵
Mohamed Salah Kamel⁵
Abdullatif Bin Muhsinah⁶
Markus Krischke⁷
Martin J Mueller⁷
Usama Ramadan
Abdelmohsen^{1,5}

¹Department of Pharmacognosy, Faculty of Pharmacy, Deraya University, Universities Zone, Minia 61111, Egypt; ²Department of Pharmacognosy, College of Pharmacy, Arab Academy for Science, Technology and Maritime Transport, Alexandria 1029, Egypt; ³Department of Pharmacognosy, Faculty of Pharmacy, Suez Canal University, Ismailia, Egypt 41522; ⁴Griffith Institute for Drug Discovery, Griffith University, Brisbane, Queensland 4111, Australia; ⁵Department of Pharmacognosy, Faculty of Pharmacy, Minia University, Minia 61519, Egypt; ⁶Department of Pharmacognosy, College of Pharmacy, King Khalid University, Abha 61441, Saudi Arabia; ⁷Department of Pharmaceutical Biology, Julius-von-Sachs Institute for Biological Sciences, University of Würzburg, Würzburg 97082, Germany

Correspondence: Martin J Mueller; Usama Ramadan Abdelmohsen
Tel +49 931 3186160; +20 86-2347759
Fax +49 931 3186182; +20 86-2369075
Email martin.mueller@biozentrum.uni-wuerzburg.de;
usama.ramadan@mu.edu.eg

Background: Hepatitis C virus (HCV) infection is a major cause of hepatic diseases all over the world. This necessitates the need to discover novel anti-HCV drugs to overcome emerging drug resistance and liver complications.

Purpose: Total extract and petroleum ether fraction of the marine sponge (*Amphimedon* spp.) were used for silver nanoparticle (SNP) synthesis to explore their HCV NS3 helicase- and protease-inhibitory potential.

Methods: Characterization of the prepared SNPs was carried out with ultraviolet-visible spectroscopy, transmission electron microscopy, and Fourier-transform infrared spectroscopy. The metabolomic profile of different *Amphimedon* fractions was assessed using liquid chromatography coupled with high-resolution mass spectrometry. Fourteen known compounds were isolated and their HCV helicase and protease activities assessed using in silico modeling of their interaction with both HCV protease and helicase enzymes to reveal their anti-HCV mechanism of action. In vitro anti-HCV activity against HCV NS3 helicase and protease was then conducted to validate the computation results and compared to that of the SNPs.

Results: Transmission electron-microscopy analysis of NPs prepared from *Amphimedon* total extract and petroleum ether revealed particle sizes of 8.22–14.30 nm and 8.22–9.97 nm, and absorption bands at λ_{max} of 450 and 415 nm, respectively. Metabolomic profiling revealed the richness of *Amphimedon* spp. with different phytochemical classes. Bioassay-guided isolation resulted in the isolation of 14 known compounds with anti-HCV activity, initially revealed by docking studies. In vitro anti-HCV NS3 helicase and protease assays of both isolated compounds and NPs further confirmed the computational results.

Conclusion: Our findings indicate that *Amphimedon*, total extract, petroleum ether fraction, and derived NPs are promising biosources for providing anti-HCV drug candidates, with nakinadine B and 3,4-dihydro-6-hydroxymanzamine A the most potent anti-HCV agents, possessing good oral bioavailability and penetration power.

Keywords: *Amphimedon*, nanoparticles, marine sponge, natural products, HCV helicase, protease, molecular docking, metabolomics

Introduction

Nanomaterials have a wide range of applications, though have many problems, accompanied by material sciences such as solar energy,¹ microelectronics² and antimicrobial activities.³ Several methods have been reported for the preparation of silver nanoparticles (SNPs), including chemical-based methods,⁴ which are not preferred, due to the toxicity

of the solvents used⁵ and reducing or stabilizing agents, such as *N,N*-dimethylformamide,⁶ that may lead to several biological and environmental hazards. Accordingly, green synthesis is preferred, because it utilizes the reducing power of natural extracts, a safer source for synthesized SNP reduction and stabilization.^{7,8} Biosynthesized silver, gold, and platinum NPs have a wide range of pharmaceutical and medical applications, such as catalysis and as antiviral and antibacterial therapeutic agents,⁹ in addition to the nonmedical applications, including the manufacturing of soap, cosmetic products, toothpaste, shampoo, and detergents.¹⁰ SNP-based materials have specific dimensions, with particle sizes of 1–100 nm.⁵ SNPs have been used in different fields, such as food packaging and water filtration, besides their multitherapeutic applications,¹¹ including antimicrobial activities.¹²

Hepatitis C virus (HCV) is an infectious liver disease that exists in many different genotypes. The HCV genome encodes three structural and six nonstructural proteins, of which NS3/4A protease and helicase are considered the most effective drug targets in current endeavors to design anti-HCV drug scaffolds. HCV infects about 170 million persons worldwide and thus acts as a viral pandemic,^{19,20} and about 3% of the world's population is infected by it.²¹ Several hepatic complications, such as steatosis, cirrhosis, and hepatocellular carcinoma, are induced by HCV infection.²² One of the major health issues in Egypt is HCV, as it infects about 14.7% of the general population.²³

The HCV genome consists of a single RNA-positive strand.²⁴ A polyprotein encoded by genomic RNA is translated by an internal ribosome, followed by cleavage through viral protease into ten mature viral proteins.²⁵ The remaining part is cleaved by viral protease, producing six nonstructural proteins, among which is NS3 protease.²⁶ The viral replication complex is formed due to these nonstructural proteins and their host factors.²⁴ Helicase exhibits an important role during RNA replication by unwinding the double RNA strand.²⁷ It has several other significant roles, such as assisting in viral replication through translation and protein processing.²⁷

Available US Food and Drug Administration–approved drugs for HCV include nucleotide derivatives, eg, sofosbuvir, and nonnucleosides, eg, boceprevir, ledipasvir, telaprevir, and simeprevir.^{28,29} These drugs inhibit the viral replication cycle that results in high rates of treatment in a shorter time.²⁹ Regardless of the available drugs offering improved viral response, some side effects have been reported during treatment with telaprevir and other protease inhibitors, such as skin rash, anemia, and gastrointestinal disorders.^{30–32} These

challenges encourage the search for new natural HCV inhibitors that can act against nonstructural proteins, such as NS3 polymerase and helicase, to inhibit virus replication.^{33–35}

The marine ecosystem is still considered a promising reservoir of unexplored bioactive natural products. Marine metabolites have been considered a potential reservoir for antiviral compounds targeting HCV, and have provided inspiring scaffolds for combinatorial chemistry to design novel antiviral agents with enhanced therapeutic potential and minimal side effects.^{38–41} Several marine sponges and their associated microbiota have been explored for anti-HCV activities.^{24,42} Harzianoic acids A and B have been isolated from the sponge-associated *Trichoderma harzianum* fungus, and showed virus-inhibitory activity via reducing HCV RNA levels.²⁹ Discorhabdins A and C and dihydrodiscorhabdin C exhibit anti-HCV activity.⁴³ Manoalide exhibits inhibitory activity against NS3 helicase, leading to inhibition of virus RNA-helicase activity.⁴⁴ Members of the genus *Amphimedon* exhibit a wide range of biological activities, as it includes different classes of metabolites, in particular pyridine alkaloids⁴⁵ of manzamine⁴⁶ and purine types,⁴⁷ as well as macrocyclic lactones/lactams,⁴⁸ ceramides, cerebrosides,⁴⁹ and fatty acids.^{50,51} In the literature, among 54 extracts from different marine organisms studied, ethyl acetate from *Amphimedon* spp. exhibited the highest anti-HCV activity,²⁴ as well as halitoxins, which are a group of toxic complexes with a 3-alkyl pyridinium structure isolated from the Red Sea sponge *Amphimedon chloros*, *Haliclona* sponges, and other marine sponges. It has been reported that 4.69 µg/mL of an organic extract of *Amphimedon* sponge containing halitoxins exhibited inhibitory activity (up to about 60%) against the West Nile Virus NS3 protease.⁵² Despite continuous attempts made to discover new drug candidates⁵³, drugs with potential anti-HCV agents have remained underexplored.¹³ However, the use of marine material in nanomedicine remains in the early stages of investigation and faces many challenges, due to difficulties in isolation and identification of the bioactive chemical entities.¹⁴ As an example of marine organisms, the marine alga *Caulerpa racemosa* has been used to synthesize SNPs with antibacterial activity against *Proteus mirabilis*.¹⁵ Moreover, marine sponge (*Haliclona exigua*) NPs exhibited activity against oral biofilm bacteria, including *Streptococcus salivarius* and *Streptococcus orulis*.¹⁶ Nanotechnology studies have also extended to developing novel antiviral therapeutic agents that interfere with viral attachment and entry during infection.¹⁷ NPs help in the treatment of HCV through their effect on HCV NS3.^{18,36,37}

This inspired us to explore the anti-HCV potential of *Amphimedon* NPs, as this has never been explored before. The anti-HCV NS3 helicase and protease activity of total extract and petroleum ether *Amphimedon* fractions were first investigated, followed by liquid chromatography (LC)–high-resolution electrospray ionization (HRESI)–mass spectrometry (MS)–based metabolic profiling for dereplication purposes. A mechanistic insight for the identified antiviral compounds was provided by the *in silico* method using molecular docking studies. The *in vitro* inhibitory potential of the isolated compounds against HCV replication was then tested. Finally, physicochemical properties of the isolated compounds were assessed by Veber's oral bioavailability rule and Lipinski's rule of five.

Methods

Sponge Material

Amphimedon marine sponge was collected from Sharm El-Shaikh (Egypt). It was then air-dried and stored at -24°C until further analysis. Voucher specimens with registration numbers BMNH 2006.7.11.1 and SAA-66 were obtained from the Natural History Museum (London, UK) and the Pharmacognosy Department (Faculty of Pharmacy, Suez Canal University, Ismailia, Egypt), respectively.

Extraction and Isolation

Freeze-dried sponge material (6 g) was extracted with methanol–methylene chloride. The resulting crude extract was fractionated between water and petroleum ether, yielding petroleum ether fraction, followed by dichloromethane, ethyl acetate, and butanol. The remaining mother liquor was then deprived of its sugars and salts with an ion-exchange resin using acetone. The organic phase in each step was separately concentrated under a vacuum, yielding petroleum ether (1 g), dichloromethane (250 mg), ethyl acetate (250 mg), butanol (1 g), and acetone (2 g) fractions. The petroleum ether fraction was chromatographed on a silica-gel column (gradient elution of petroleum ether: EtOAc, then EtOAc), followed by methanol, which was then chromatographed on a Sephadex LH-20 (Merck, Bremen, Germany) using methanol:water as eluting solvent, and final purification on semipreparative HPLC with acetonitrile (MeCN) and water as mobile phase complemented by 0.05 percent trifluoroacetic acid with a gradient elution of 10% MeCN– H_2O to 100% MeCN over 30 minutes at a flow rate of 5 mL/min to yield compounds (1–14).

Synthesis of Silver SNPs

Total extract (0.002g) and petroleum ether fraction were individually dissolved in 1 mL DMSO. This was followed by the addition of 0.4 mL of each extract to 10 mL 1mM AgNO_3 at room temperature.

Characterization of Synthesized SNPs by Ultraviolet-Visible Spectrometry, Transmission Electron Microscopy, and Fourier-Transform Infrared Spectroscopy

SNP synthesis was detected by ultraviolet (UV)-visible spectrometry using a double-beam V630 (Jasco, Japan), Fourier-transform infrared (FTIR) using an FTIR-8400S, IR Prestige 21, and IR Affinity 1 (Shimadzu, Japan), and transmission electron microscopy (TEM) using a JEM-1010, (Jeol, USA).¹¹

Metabolic Analysis

LCMS was carried out using a Synapt G2 HDMS quadrupole time-of-flight hybrid mass spectrometer (Waters, Milford, USA). The sample (2 μL) was injected into the BEH C_{18} column, adjusted to 40°C , and connected to the guard column. A gradient elution of mobile phase was used, starting from no solvent A and 0.1% formic acid in water to 100% acetonitrile as solvent B. MZmine 2.12 was employed for differential investigation of MS data, followed by converting the raw data into positive and negative files in mzML format with ProteoWizard.¹³

Anti-HCV Helicase and Protease Assay

Assay buffer (4 μL 25 mM MOPS pH 6.5, 1.25 mM MgCl_2 , 0.1 mM DTT, 12.5 mM Tween 20, 6 $\mu\text{g}/\text{mL}$ BSA) containing 5.56 nM NS3 substrate and 13.89 nM NS3 helicase fragments was distributed into wells of a 1,536 mL plate. The compounds tested (55 μL) were dissolved in DMSO. In each well, 110 mM thioflavin S or 0.8% of DMSO and 1 mL 5 mM ATP were added. Fluorescence intensity was measured after 1 hour of incubation at 25°C on a ViewLux (PerkinElmer). The ratio between RFU values obtained at t_0 (RFU $_{t_0}$) and t_{60} (RFU $_{t_{60}}$), named Ratio_RFU, was calculated: $\text{Ratio_RFU} = \text{RFU}_{t_{60}}/\text{RFU}_{t_0}$. The percentage of inhibition was calculated. The activity score was classified according to the potency, ie, the most potent extract was that possessing the highest activity scores. Activity-score ranges for active and inactive extracts were 82–100 and 0–79, respectively.

Chemicals and Reagents

NS3 helicase fragments and assay buffer were supplied by Assay Provider, and 1,536-well plates (part 789,173) by Greiner. MOPS (part BP308-100), ATP (part BP413-25), and magnesium chloride (part BP214-500) were purchased from Fisher BioReagents. Thioflavin S (part T1892) was procured from Sigma-Aldrich, and a Cy5/quencher-labeled molecular beacon (custom-synthesized) was procured from Integrated DNA Technologies.

Assays of Activity of Isolated Compounds Against HCV

HCV cells were inoculated at 26×10^4 cells per well in a 48-well plate 24 hours before assays (Reblikon, Mainz, Germany) were conducted. Concentrations of 1–200 μM of each tested sample were prepared and a luciferase-assay system (Promega) utilized to measure luciferase activity. The resulting luminescence was measured with a luminescence plate reader (PerkinElmer) and this alternative to the level of the HCV replicon.⁵⁴

Docking Studies

Docking simulations were performed using Molecular Operating Environment (MOE 2014.0901; Chemical Computing Group, Montreal, QC, Canada) on the compounds identified in *Amphimedon* spp., in addition to paritaprevir and ribavirin 5'-triphosphate (helicase inhibitor), for the sake of comparison to their inhibitory potential.⁵⁵ We drew two-dimensional structures of the known compounds with ChemSketch, then docked into the rigid binding pocket of HCV NS3–4A protease–helicase in complex with a macrocyclic protease inhibitor (PDB 4A92), HCV NS3/NS4A protease complexed with BI 201,335 (PDB 3P82), and HCV NS3 helicase with {6-(3,5-aminophenyl)-1-[4-(propane-2-yl)benzyl]-1H-indol-3-yl} acetic acid as a bound inhibitor (PDB4WXR). The 3-D crystal structure of these three enzymes was downloaded from Protein Data Bank.^{55,56}

Results

Anti-HCV NS3 Helicase and Protease Activities

The total extract and the derived fractions of *Amphimedon* were tested for their HCV NS3 helicase and protease activities, and only the total extract, as well as the petroleum ether fraction, exhibited inhibitory potential against HCV NS3 helicase and protease (Table 1). This led us to

Table 1 In vitro Anti-NS3 Helicase and Protease Activities of Total Extract and Fractions of *Amphimedon* sp.

	IC ₅₀ , $\mu\text{g/mL}$	
	NS3 helicase	NS3 protease
Petroleum ether	0.296063	3.875308
Total extract	2.066837	13.29783
Butanol	2.346521	35.29088
Ethyl acetate	2.782707	43.69913
DCM	11.09016	29.79358

use *Amphimedon* total extract and petroleum ether fraction in the formation of SNPs, which showed a better anti-HCV NS3 helicase and protease action (Table 2). The bioactive petroleum ether fraction was then subjected to further chromatographic separation with different chromatographic techniques to yield 14 known compounds (1–14, Figure 1), which were identified based on HRESI mass spectra in comparison to literature data.

Metabolomic Profiling of Total Extract and Petroleum Ether Fraction of *Amphimedon*

The crude extract of freeze-dried *Amphimedon* was subjected to dereplication of secondary metabolites using LC-HR-ESIMS (Table S1 and Figure 2). Twelve compounds belonging to different chemical classes were identified. This revealed the richness of this marine sponge.

Characterization of Synthesized SNPs of *Amphimedon* Total Extract and Petroleum Ether Fraction

Both the total extract and petroleum ether fraction of *Amphimedon*, possessing the highest activity, were used in green SNP synthesis. The total extract and petroleum

Table 2 In vitro Anti-NS3 Helicase and Protease Activities of the SNP Total Extract and Petroleum Ether Fraction of *Amphimedon* sp.

	IC ₅₀ , $\mu\text{g/mL}$	
	NS3 Helicase	NS3 Protease
Petroleum ether	0.11±0.62	2.38±0.57
Total extract	1.52 ±1.18	9.76±0.58
AgNO ₃	77.72 ±4.57	52.67±0.33
Telaprevir (375 mg Tab)	—	4.77±0.26
Ribavirin	4.66±0.29	—

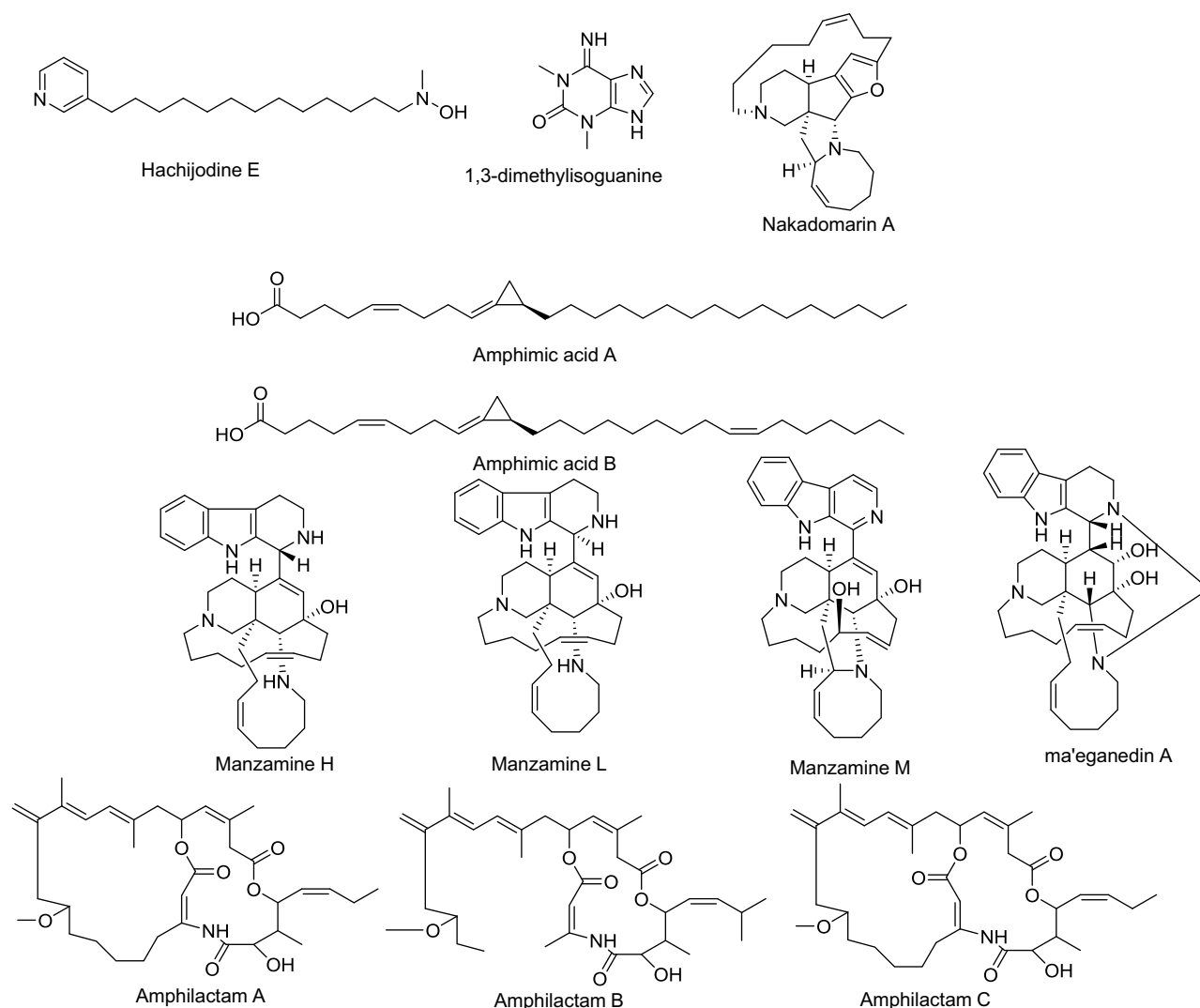


Figure 1 Compounds identified and dereplicated from high-resolution mass-spectra data sets of *Amphimedon* sp.

ether fraction of *Amphimedon* were treated with 1 mM AgNO_3 , and caused the color to change to reddish brown, indicating SNP synthesis (Figure S1). NPs of total extract and petroleum ether fraction appeared spherical, with particle sizes of 8.22–14.30 nm and 8.22–9.97 nm, respectively, on TEM analysis (Figure 3).

UV-Visible Characterization of Synthesized SNPs of *Amphimedon* Total Extract and Petroleum Ether fraction

SNP formation was controlled by UV light at a wavelength of 200–600 nm. SNPs were formed by the addition of 0.4 mL *Amphimedon* total extract to 10 mL AgNO_3 (1 mM) and 0.6 mL petroleum ether extract of sponge extract in DMSO to of 10 mL silver (1 mM), then we used UV

spectra to analyze the synthesized NPs. The total extract and petroleum ether fraction exhibited absorbance bands at 450 and 415 nm, respectively. This proved SNP synthesis (Figure 4).

FTIR Characterization of Synthesized SNPs

FTIR was used in characterization of functional groups' adherence to SNP surfaces. The FTIR spectrum showed peaks at 3,432.67, 3,419.17, 2,974.66, 2,930.31, 1,449.24, 876.488, and 872.631 cm^{-1} revealing the presence of different phytochemicals, ie, alkaloids, acids, and phenolic compounds. The peaks at 3,200–3,500 cm^{-1} confirmed the presence of O–H stretching of alcohols and phenolic compounds with strong hydrogen bonds, in addition to N–

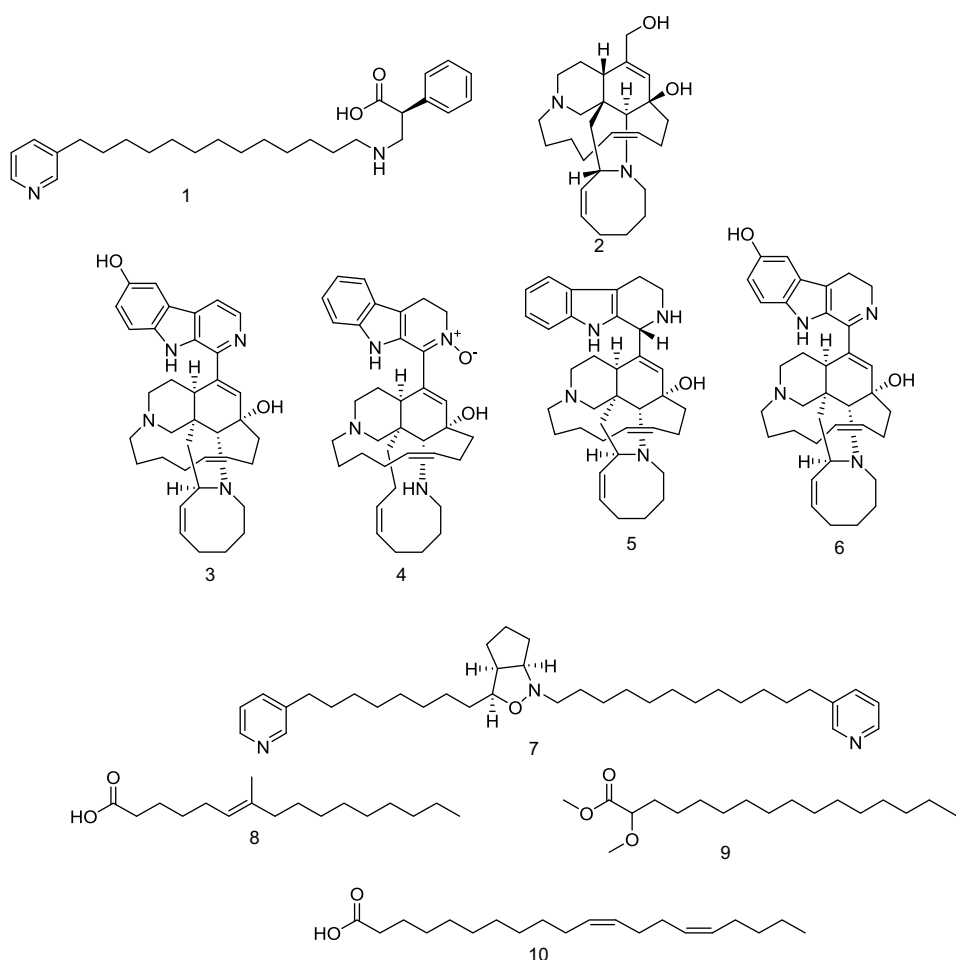


Figure 2 Structures of isolated compounds 1–14.

H group stretching. Peaks appearing at $2,800\text{--}3,000\text{ cm}^{-1}$ were characteristic of C–H and aldehydic C–H stretching. O–H stretching in carboxylic acid appeared at $2,700\text{--}3,350\text{ cm}^{-1}$. C–C stretching in an aromatic ring showed characteristic peaks in the region of $1400\text{--}1500\text{ cm}^{-1}$, which included C–H bending of alkanes at $1450\text{--}1470\text{ cm}^{-1}$. However, C–H aromatics were detected at $675\text{--}900\text{ cm}^{-1}$ (Figure 5). These groups indicated the stability of the synthesized NPs.

Molecular Docking

The relative inhibitory potential of the tested compounds from *Amphimedon* was explored against HCV NS3 protease and helicase enzymes using an in silico approach via molecular docking. The docking study showed that most of the identified compounds were able to interact with the active sites of both HCV NS3 protease and helicase domains, but with differential binding affinity, expressed as docking S-scores (Table 3 and Figure 6). The potential

binding interactivity between protease and helicase domains of HCV NS3 is shown in Figures S2 and S3. Pynodemin D (7) and nakinadine B (1) were potential anti-HCV drug candidates, owing to their noticeably strong inhibitory activity against NS3/4A protease–helicase enzyme. In vitro investigation for the tested compounds showed that the results matched those of the in silico study: pynodemin D showed the highest inhibitory activity against the HCV replicon, then nakinadine B, and finally 3,4-dihydro-6-hydroxymanzamine A, while the rest of the compounds displayed weak activity.

Lipinski Properties

The four Lipinski properties, in addition to two additional descriptors of topological polar surface area (tPSA) and numbers of rotation bonds of the 14 isolated compounds were analyzed (Table S2). Veber's oral bioavailability rule was estimated, and included two additional parameter ranges (tPSA $\leq 140\text{ \AA}$, number of rotatable bonds ≤ 10).

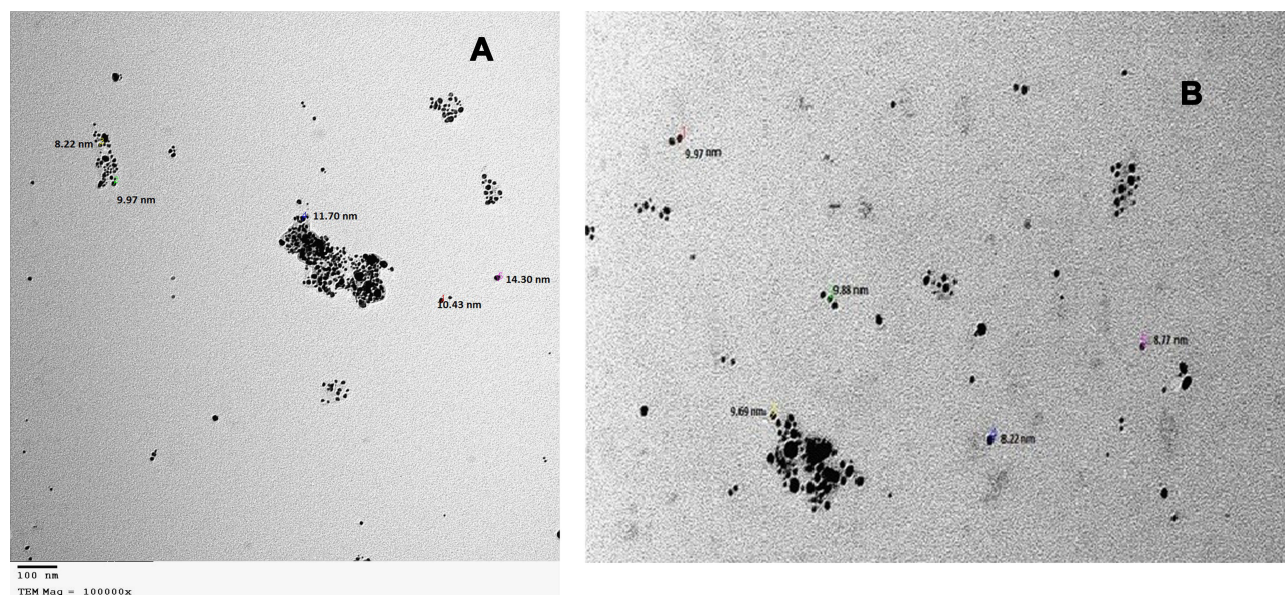


Figure 3 TEM for shape and size of produced SNPs of (A) total extract of *Amphimedon* sp. and (B) Petroleum ether fraction of *Amphimedon*. **Abbreviations:** TEM, transmission electron microscopy; SNPs, silver NPs

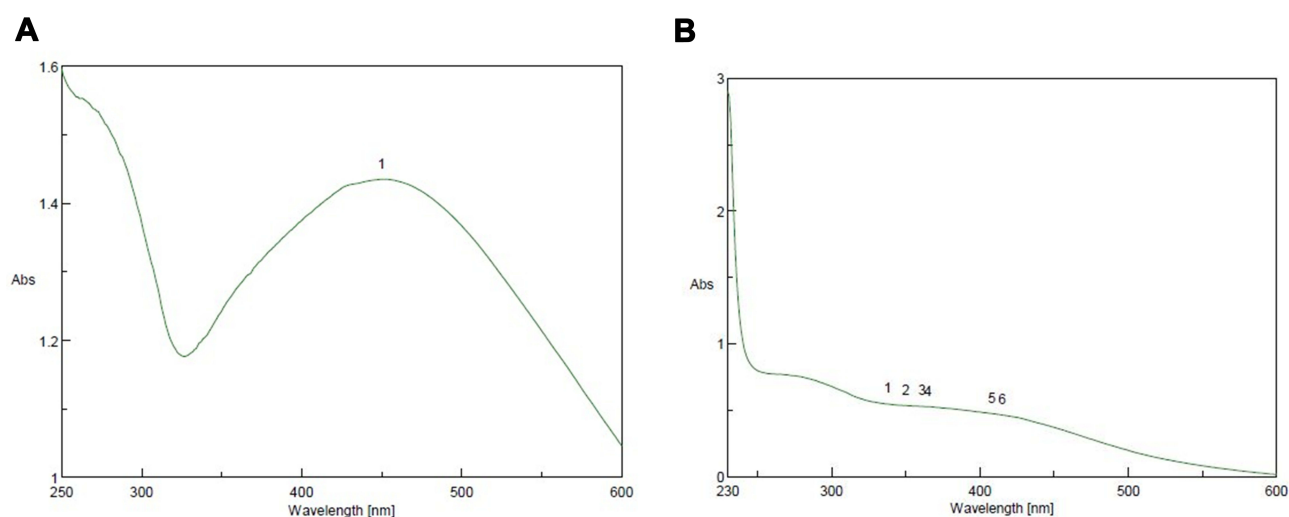


Figure 4 Ultraviolet-visible spectra analysis and color intensity of biosynthesized SNPs of (A) petroleum ether fraction of *Amphimedon* spp. and (B) total extract of *Amphimedon*.

The isolated compounds were tested for their oral bioavailability in humans, and about 71% (ten of 14) of the isolated metabolite followed Lipinski's rule of five with less than one violation, and the most active anti-HCV drugs perfectly obeyed the rule of five and the rule of PSA.

Discussion

Synthesis of SNPs was detected by the development of a reddish brown color at 37°C.⁵⁷ The actual mechanism of SNP reduction has previously been reported.⁵⁷ Both the spherical shape and size of 8.22–14.30 nm confirmed the

formation of NPs, as measured by TEM. FTIR analysis revealed the presence of various phytochemical classes in the sponge with the ability to react with silver ions through their functional groups, leading to NP reduction. As previously reported, NPs may provide a successful tool in the treatment of HCV,¹⁸ given their effect against HCV NS3. The green synthesized NPs of total extract and petroleum ether fraction exhibited activity against HCV NS3 helicase (IC_{50} 0.11±0.62 and 1.52±1.18) and protease (IC_{50} 2.38±0.57 and 9.76±0.58), while silver nitrate NPs as controls exhibited activity against HCV NS3 helicase and protease

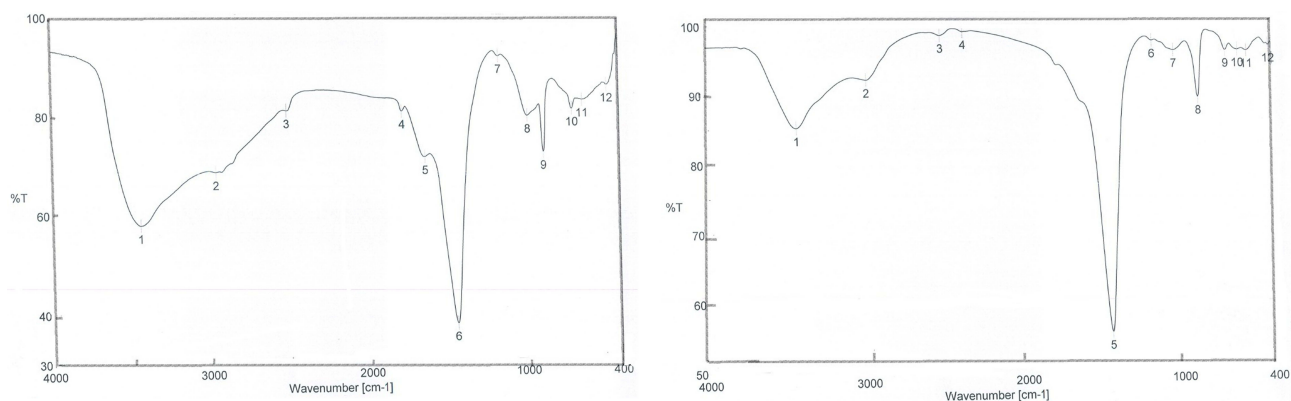


Figure 5 FTIR spectra after synthesis of nanoparticles of (A) petroleum ether fraction of *Amphimedon* sp. and (B) total extract of *Amphimedon*.

(IC_{50} 77.72 \pm 4.57 and 52.67 \pm 0.33), respectively. This showed the power of the total extract and petroleum ether fraction synthesized NPs of *Amphimedon*

HR-LCMS-based metabolite profiling of sponge extracts was conducted to identify putative constituents responsible for the activity. Dereplicated identified compounds shown in Figure 1 belonged to a diverse range of phytochemical classes, such as amphimic acids (A and B)⁵⁰ and alkaloids with various subclasses, eg,

Table 3 Docking Scores (kcal/Mol) of the 14 Tested Compounds, Paritaprevir, and Ribavirin 5'-Triphosphate Against Full-Length HCV NS3-4A Protease–Helicase (4A92), HCV NS3/NS4A Protease (3P82), and HCV NS3 Helicase (4WXR)

	S-Score		
	4A92	3P82	4WXR
Methyl 2-methoxyhexadecanoate	-5.07427	-4.75656	-5.51035
Icricinol A	-5.34033	-5.30877	-5.47285
6-hydroxymanzamine A	-5.49333	-5.37674	-6.26323
Pyrinodemin D	-6.98161	-5.14564	-7.64613
7-methyl-6-hexadecenoic acid	-5.09503	-4.49901	-5.4961
Amphimedine	-5.51757	-4.60604	-5.1061
Amphimedoside C	-5.84524	-5.22292	-5.84337
Keramaphidin B	—	—	—
20-hepacosenoic acid	-5.31298	-5.68273	-5.73547
3,4-dihydro-6-hydroxymanzamine A	-6.25434	-5.9257	-6.62751
3,4-dihyromanzamine A, J N-oxide	-6.26893	-4.72766	-5.56533
Nakinadine B	-6.4761	-6.17759	-6.80996
11,15-icosadienoic acid	-5.61213	-4.6286	-5.78322
Manzamine D	-5.62775	-5.10746	—
Paritaprevir	—	-5.95468	—
Ribavirin 5'-triphosphate	—	—	-5.94529

manzamine compounds, such as manzamine L,⁵⁸ H, and M, ma'eganedin A⁵⁹ and nakadomarin A,⁶⁰ in addition to purine alkaloid (1,3-dimethylisoguanine)⁶¹ and pyridine alkaloids, ie, hachijodine E and⁶² amphilactams A, B, and C.⁴⁸ Total extract and different fractions of *Amphimedon* were assayed in vitro against HCV NS3 helicase and protease, and the petroleum ether fraction was revealed to exhibit the most potent activity (Table 1). That is why we used this fraction in subsequent chromatographic separation with different techniques. Fourteen compounds (1–14), shown in Figure 2, were identified based on their HR-ESIMS and comparison with the literature: nakinadine B⁶³ (1), orcinol A⁶⁴ (2), 6-hydroxymanzamine A⁶⁵ (3), 3,4-dihyromanzamine A, J N-oxide⁶⁵ (4), manzamine D⁵⁸ (5), 3,4-dihydro-6-hydroxymanzamine A⁶⁶ (6), pyrinodemin D⁴⁵ (7), 7-methyl-6-hexadecenoic acid⁶⁷ (8), methyl 2-methoxyhexadecanoate⁶⁸ (9), 11,15-icosadienoic acid⁶⁷ (10), 20-hepacosenoic acid⁶⁹ (11), amphimedoside C⁷⁰ (12), keramaphidin B⁷¹ (13), and amphimedine⁷² (14).

Docking studies showed that nakinadine B (1) possessed the lowest S-score (strongest binding affinity) and ranked top of the identified compounds, followed by 3,4-dihydro-6-hydroxymanzamine A (6) and 20-hepacosenoic acid (11). Nakinadine B (1) achieved hydrogen bonding with Thr40 of the protease domain, and 3,4-dihydro-6-hydroxymanzamine A (6) had an arene–hydrogen interaction with His528 and hydrogen bonding with Cys159. 20-Hepacosenoic acid (11) showed hydrogen bonding with Arg109. Pyrinodemin D (7), nakinadine B (1), 3,4-dihydro-6-hydroxymanzamine A (6), and 6-hydroxymanzamine A (3) were noted to possess the lowest docking scores in binding with HCV NS3 helicase enzyme among the studied compounds. Gly277 and Arg512 residues of the enzyme showed arene–H and H bonding with

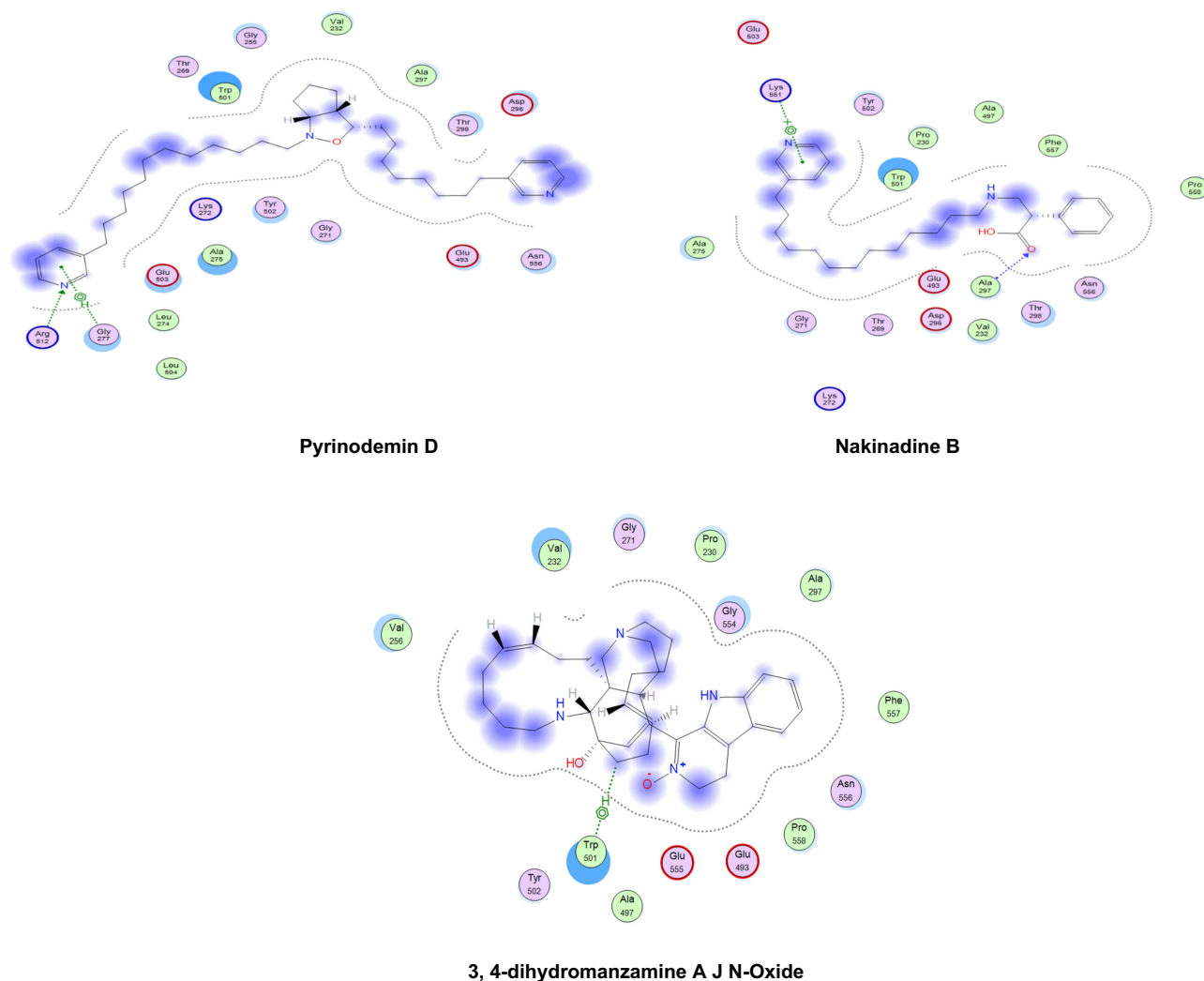


Figure 6 2-D interaction diagrams of docked compounds and ribavirin 5'-triphosphate (**M**) with the active sites of HCV NS3 helicase (4WXR). Green arrows represent side-chain acceptor/donor; blue arrows represent backbone acceptor/donor; blue shadows represent ligand exposure.

pyrinodemin D (**7**), respectively. However, the two enzyme residues Lys551 and Ala297 showed arene–cation and H-bonding with pyrinodemin D (**7**). 6-Hydroxymanzamine A (**3**) showed an arene–H bond with Trp501 and an H-bond with Glu493.

To explore the combined protease and helicase–inhibition activity of the studied compounds, they were further docked against HCV NS3–4A protease–helicase ([Figure S4](#)). Pyrinodemin D (**7**), nakinadine B (**1**), 3,4-dihydropyranzamine A, J *N*-oxide (**4**), and 3,4-dihydro-6-hydroxymanzamine A (**6**) possessed the most active inhibitors on the basis of their docking scores. Pyrinodemin D (**7**) had the strongest binding affinity with the helicase enzyme through H-bonding with Gly137 and Arg 123, followed by nakinadine B (**1**), which showed two arene–H bonds with Gln41 and Cys159 and H-bonding with Ala157. However, 3,4-dihydropyranzamine

A, J *N*-oxide (**4**) showed H-bonding with His57 ([Figure 6](#)). His57 and Lys136 showed arene–H bonding with 3,4-dihydro-6-hydroxymanzamine A (**6**). It has been reported that the existence of the protease domain in full-length NS3 can modify substrate selectivity and improve the unwinding and binding of RNA.⁷³ Also, the helicase domain has been reported to enhance protease-domain activity when existing in full-length HCV NS3 protein,⁷⁴ as exemplified by polyuracil, which has been reported to stimulate protease activity of full-length NS3 but not the isolated protease domain.⁷⁵ Such activity was witnessed in our study with the compounds pyrinodemin D (**7**), and 3,4-dihydropyranzamine A, J *N*-oxide (**4**), which had weak binding affinity with HCV NS3 protease enzymes, but were among the most active compounds inhibiting the full-length NS3–4A protease–helicase ([Table 1](#)). Additionally, it was concluded that protease improved helicase activity and

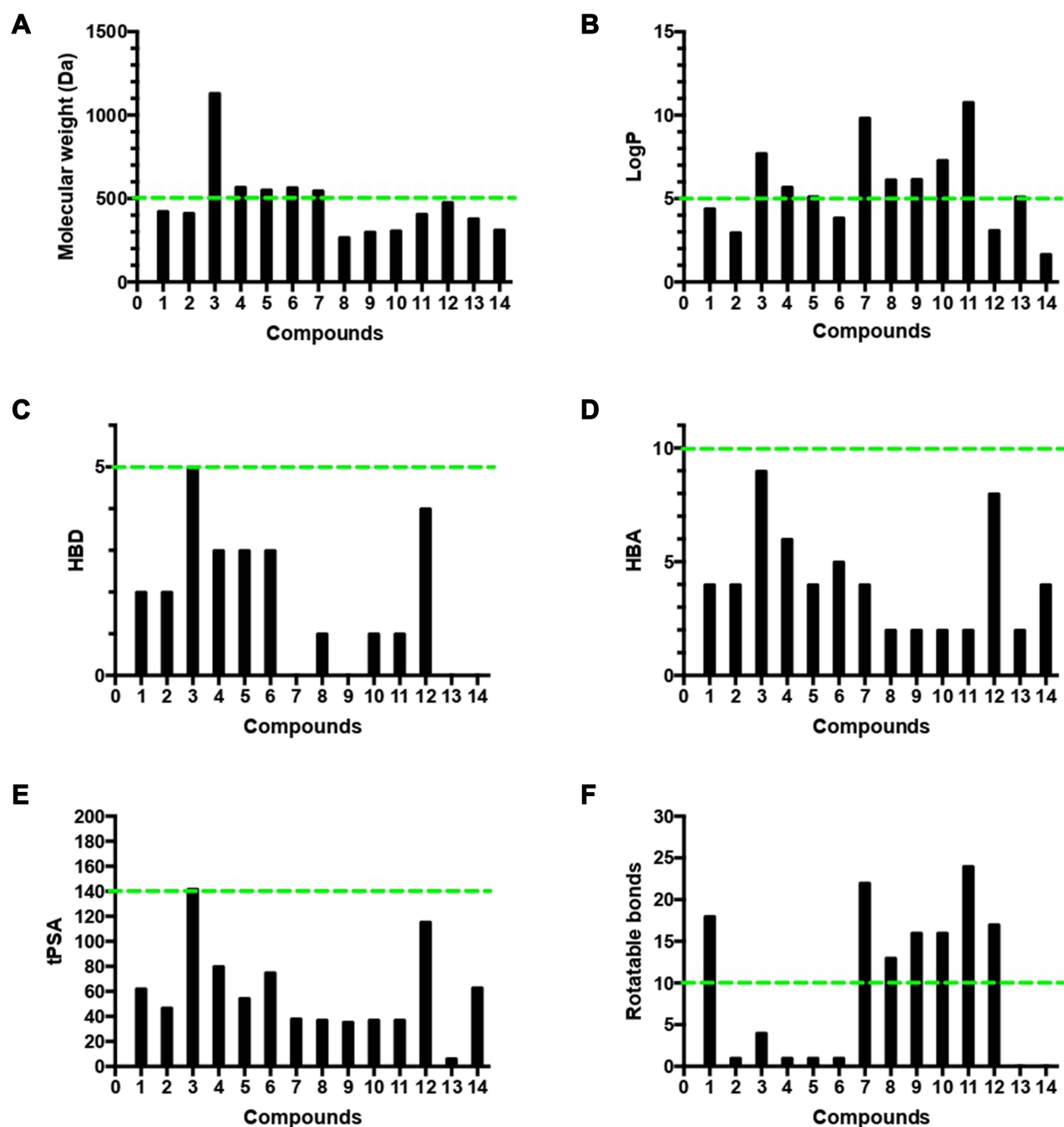


Figure 7 Analysis of physicochemical properties for the 14 isolated compounds by (A) molecular weight, (B) log P, (C) HBD, (D) HBA, (E) tPSA, and (F) number of rotatable bonds. The green line indicates the maximum desirable value for oral bioavailability defined by Lipinski's rule of five and Veber's oral bioavailability rule.

vice versa,⁷⁴ which might have contributed to the increased binding affinity of pyrinodemin D (7) with the full-length NS3-4A protease-helicase, despite exhibiting weak interactions with the isolated protease domain but strong inhibitory activity with the isolated helicase domain.

From this study, we can conclude that pyrinodemin D (7) and nakinadine B (1) can serve as potential anti-HCV drug candidates, owing to their observed strong

inhibitory activity against the NS3-4A protease-helicase enzyme. The *in silico* results were substantiated by *in vitro* assays in which inhibitory activity against HCV replicons was recorded for pyrinodemin D, nakinadine B, and 3,4-dihydro-6-hydroxymanzamine A (IC₅₀ 5.8, 15.6, and 17.2 µg/mL, respectively) the most active compounds. However, the rest of the compounds exhibited IC₅₀ values >200 µg/mL.

Accordingly, our results highlighted pyrinodemin D, nakinadine B, and 3,4-dihydro-6-hydroxymanzamine A as the most promising anti-HCV drug leads. Since therapeutic agents must possess appropriate physicochemical properties for cell penetration and delivery to the target organ, we analyzed the four Lipinski properties and two additional descriptors — tPSA and numbers of rotation bonds for the 14 isolated compounds — to assess their oral bioavailability in humans (Table S2, Figure 7). We estimated Lipinski's rule of five, which defines four simple physicochemical parameter ranges (MW \leq 500, logP \leq 5, HBD \leq 5, and HBA \leq 10)⁷⁶ for orally active compounds and Veber's oral bioavailability rule, which includes two additional parameter ranges (tPSA \leq 140 Å, number of rotatable bonds \leq 10).⁷⁷ The results indicated that 71% (ten of 14) of the isolated compounds followed Lipinski's rule of five with less than one violation: MW \leq 500 Da (nine of 14, Figure 7A), logP \leq 5 (five of 14, Figure 7B), HBD \leq 5 (14 of 14, Figure 7C), HBA \leq 10 (14 of 14, Figure 7D), tPSA \leq 140 Å (13 of 14) (Figure 7E), and number of rotation bonds \leq 10 (five of 14) (Figure 7F). The active anti-HCV compound nakinadine B (1) was found to perfectly obey the rule of five and the rule of tPSA, and 3,4-dihydro-6-hydroxymanzamine A (6) violated only the MW rule with 566 Da, indicating their high potential to be promising anti-HCV drug candidates with good oral bioavailability and penetration power. However, the most active compound, pyrinodemin D (7), violated both the MW and logP rules, indicating its poor oral bioavailability.

Conclusion

This study presented a green synthesis of SNPs from total extract and petroleum ether fraction of *Amphimedon* with potent in vitro anti-HCV NS3 helicase and protease activity. A diverse phytochemical class of natural products was identified using LCMS-based metabolic investigation, followed by the identification of 14 known compounds via bioassay-guided isolation. Docking studies of the identified compounds postulated their mechanism of action, which was further evidenced by in vitro assays. Among the *Amphimedon* sponge phytochemicals, nakinadine B and 3,4-dihydro-6-hydroxymanzamine A were noted as promising anti-HCV drug candidates, warranting future clinical investigation.

Acknowledgment

This publication was funded by the German Research Foundation (DFG) and the University of Würzburg under the funding program Open Access Publishing. The authors

are grateful to Michelle Kelly at the National Institute of Water and Atmospheric Research (NIWA), Auckland, New Zealand for taxonomic identification of the sponge samples. Thanks are also due to the Egyptian Environmental Affairs Agency (EEAA) for facilitating sample collection along the coasts of the Red Sea. We thank Maria Lesch (University of Würzburg) for her help in the laboratory.

Disclosure

Professor Dr Ronald J Quinn reports grants from the Australian Research Council during the conduct of the study. The authors declare that they have no other conflicts of interest.

References

1. Zhao T, Sun R, Yu S, et al. Size-controlled preparation of silver nanoparticles by a modified polyol method. *COLLOID SURF A PHYSICOCHEM ENG ASP*. 2010;366(1–3):197–202. doi:10.1016/j.colsurfa.2010.06.005
2. Sun Y, Mayers B, Herricks T, Xia Y. Polyol synthesis of uniform silver nanowires: a plausible growth mechanism and the supporting evidence. *Nano Lett*. 2003;3(7):955–960. doi:10.1021/nl034312m
3. Du W-L, Niu -S-S, Xu Y-L, Xu Z-R, Fan C-L. Antibacterial activity of chitosan tripolyphosphate nanoparticles loaded with various metal ions. *Carbohydr*. 2009;75(3):385–389. doi:10.1016/j.carbpol.2008.07.039
4. Sinha S, Pan I, Chanda P, Sen SK. Nanoparticles fabrication using ambient biological resources. *J Appl Biosci*. 2009;19:1113–1130.
5. Amin M, Anwar F, Janjua MRSA, Iqbal MA, Rashid U. Green synthesis of silver nanoparticles through reduction with solanum xanthocarpum L. berry extract: characterization, antimicrobial and urease inhibitory activities against helicobacter pylori. *Int J Mol Sci*. 2012;13(8):9923–9941. doi:10.3390/ijms13089923
6. Pastoriza-Santos I, Liz-Marzán LM. Formation of PVP-protected metal nanoparticles in DMF. *Langmuir*. 2002;18(7):2888–2894. doi:10.1021/la015578g
7. Zou J, Zhang F, Huang J, Chang PR, Su Z, Yu J. Effects of starch nanocrystals on structure and properties of waterborne polyurethane-based composites. *Carbohydr*. 2011;85(4):824–831. doi:10.1016/j.carbpol.2011.04.006
8. Mondal AK, Mondal S, Samanta S, Mallick S. Synthesis of eco-friendly silver nanoparticle from plant latex used as an important taxonomic tool for phylogenetic interrelationship advances in bioresearch vol. 2. *Synthesis*. 2011;31:33.
9. Sekhar EC, Rao K, Rao KMS, Alisha SB. A simple biosynthesis of silver nanoparticles from syzygium cumini stem bark aqueous extract and their spectrochemical and antimicrobial studies. *J Appl Pharm*. 2018;8(01):073–079.
10. Singh M, Kalaivani R, Manikandan S, Sangeetha N, Kumaraguru AK. Facile green synthesis of variable metallic gold nanoparticle using *Padina gymnospora*, a brown marine macroalgae. *Appl Nanoscience*. 2013;3(2):145–151. doi:10.1007/s13204-012-0115-7
11. Haggag EG, Elshamy AM, Rabeh MA, et al. Antiviral potential of green synthesized silver nanoparticles of *lampranthus coccineus* and *malephora lutea*. *Int J Nanomedicine*. 2019;14:6217–6229. doi:10.2147/IJN.S214171
12. El-Nour KMA, Eftaiha A, Al-Warthan A, Ammar RA. Synthesis and applications of silver nanoparticles. *Arab J Chem*. 2010;3(3):135–140. doi:10.1016/j.arabjc.2010.04.008

13. Shady NH, Fouad MA, Ahmed S, et al. A new antitrypanosomal alkaloid from the Red Sea marine sponge *Hyrtios* sp. *J Antibiot (Tokyo)*. 2018;71(12):1036–1039. doi:10.1038/s41429-018-0092-5
14. Srividhya S, Chellaram C. Role of marine life in nanomedicine. *Ind J Innov Develop*. 2012;1(S8):31–33.
15. Kulkarni SR, Dikshit M. Indian marine pharmacology: a sneak peek into the ecosystem. *Proc Indian Natl Sci Acad B*. 2018;84(1):281–300.
16. Arya G, Sharma N, Mankamna R, Nimesh S. Antimicrobial silver nanoparticles: future of nanomaterials. In: *Microbial Nanobionics*. Springer. 2019;89–119.
17. El-Gaied HAAA. Antiviral evaluation of secondary metabolites derived from actinomycetes conjugated to silver nanoparticles. *CU Theses*. 2018.
18. Ryoo S-R, Jang H, Kim K-S, et al. Functional delivery of DNzyme with iron oxide nanoparticles for hepatitis C virus gene knockdown. *Biomaterials*. 2012;33(9):2754–2761. doi:10.1016/j.biomaterials.2011.12.015
19. Schiering N, D'Arcy A, Villard F, et al. A macrocyclic HCV NS3/4A protease inhibitor interacts with protease and helicase residues in the complex with its full-length target. *PNAS*. 2011;108(52):21052–21056. doi:10.1073/pnas.1110534108
20. Lauer GM, Walker BD. Hepatitis C virus infection. *N Engl J Med*. 2001;345(1):41–52. doi:10.1056/NEJM200107053450107
21. Chlibek R, Smetana J, Sosovickova R, et al. Prevalence of hepatitis C virus in adult population in the Czech Republic - time for birth cohort screening. *PLoS One*. 2017;12(4):e0175525–e0175525. doi:10.1371/journal.pone.0175525
22. Licata A, Minissale MG, Montalto FA, Soresi M. Is vitamin D deficiency predictor of complications development in patients with HCV-related cirrhosis? *Intern Emerg Med*. 2019;14(5):735–737. doi:10.1007/s11739-019-02072-w
23. Gaballah AM, Esawy MM. Comparison of 2 different antibody assay methods, Elecsys Anti-HCVII (Roche) and Vidas Anti-HCV (Biomérieux), for the detection of antibody to hepatitis C virus in Egypt. *Diagn Microbiol Infect Dis*. 2018;92(2):107–111. doi:10.1016/j.diagmicrobio.2018.05.013
24. Fujimoto Y, Salam KA, Furuta A, et al. Inhibition of both protease and helicase activities of hepatitis C virus NS3 by an ethyl acetate extract of marine sponge *Amphimedon* sp. *PLoS One*. 2012;7(11):e48685. doi:10.1371/journal.pone.0048685
25. Moriishi K, Matsuura Y. Exploitation of lipid components by viral and host proteins for hepatitis C virus infection. *Front Microbiol*. 2012;3:54. doi:10.3389/fmicb.2012.00054
26. Hong TT, Dat TTH, Cuc NTK, Cuong PV. Mini-review protease inhibitor (PI) and Pis from sponge-associated microorganisms. *Vietnam J Sci Technol*. 2018;56(4):405. doi:10.15625/2525-2518/56/4/10911
27. Belon CA, Frick DN. *Helicase Inhibitors as Specifically Targeted Antiviral Therapy for Hepatitis C*. 2009.
28. Jensen DM. A new era of hepatitis C therapy begins. *N Engl J Med*. 2011;364(13):1272–1274. doi:10.1056/NEJMe1100829
29. Li B, Li L, Peng Z, et al. Harzianoic acids A and B, new natural scaffolds with inhibitory effects against hepatitis C virus. *Bioorg Med Chem*. 2019;27(3):560–567. doi:10.1016/j.bmc.2018.12.038
30. Lange CM, Sarrazin C, Zeuzem S. specifically targeted anti-viral therapy for hepatitis C—a new era in therapy. *Aliment Pharmacol Ther*. 2010;32(1):14–28. doi:10.1111/j.1365-2036.2010.04317.x
31. Feld JJ, Hoofnagle JH. Mechanism of action of interferon and ribavirin in treatment of hepatitis C. *Nature*. 2005;436(7053):967. doi:10.1038/nature04082
32. Kjellin M, Wesslén T, Löfblad E, Lennerstrand J, Lannergård A. The effect of the first-generation HCV-protease inhibitors boceprevir and telaprevir and the relation to baseline NS3 resistance mutations in genotype 1: experience from a small Swedish cohort. *Ups J Med Sci*. 2018;123(1):50–56. doi:10.1080/03009734.2018.1441928
33. Chen C, Qiu H, Gong J, et al. (–)-Epigallocatechin-3-gallate inhibits the replication cycle of hepatitis C virus. *Arch Virol*. 2012;157(7):1301–1312. doi:10.1007/s00705-012-1304-0
34. Gonzalez O, Fontanes V, Raychaudhuri S, et al. The heat shock protein inhibitor Quercetin attenuates hepatitis C virus production. *Hepatology*. 2009;50(6):1756–1764. doi:10.1002/hep.23232
35. Bachmetov L, Gal-Tanamy M, Shapira A, et al. Suppression of hepatitis C virus by the flavonoid quercetin is mediated by inhibition of NS3 protease activity. *J Viral Hepatitis*. 2012;19(2):e81–e88. doi:10.1111/j.1365-2893.2011.01507.x
36. Li Y, Yu S, Liu D, Proksch P, Lin W. Inhibitory effects of polyphenols toward HCV from the mangrove plant *Excoecaria agallocha* L. *Bioorg Med Chem Lett*. 2012;22(2):1099–1102. doi:10.1016/j.bmcl.2011.11.109
37. Sahuc M-E, Sahli R, Rivière C, et al. Dehydrojuncusol, a natural phenanthrene compound extracted from *Juncus maritimus* is a new inhibitor of hepatitis C virus RNA replication. *J Virol*. 2019; JVI:02009–02018.
38. Sepčić K, Kaufenstein S, Mebs D, Turk T. Biological activities of aqueous and organic extracts from tropical marine sponges. *Mar Drugs*. 2010;8(5):1550. doi:10.3390/md8051550
39. Shady N, El-Hossary E, Fouad M, Gulder T, Kamel M, Abdelmohsen U. Bioactive natural products of marine sponges from the genus *Hyrtios*. *Molecules*. 2017;22(5):781. doi:10.3390/molecules22050781
40. Abdelmohsen UR, Balasubramanian S, Oelschlaeger TA, et al. Potential of marine natural products against drug-resistant fungal, viral, and parasitic infections. *Lancet Infect Dis*. 2017;17(2):e30–e41. doi:10.1016/S1473-3099(16)30323-1
41. Liu M, El-Hossary EM, Oelschlaeger TA, Donia MS, Quinn RJ, Abdelmohsen UR. Potential of marine natural products against drug-resistant bacterial infections. *Lancet Infect Dis*. 2019.
42. Ahmed EF, Rateb ME, Abou El-Kassem LT, Hawas UW. Anti-HCV protease of diketopiperazines produced by the Red Sea sponge-associated fungus *Aspergillus versicolor*. *Appl Biochem Biotechnol*. 2017;53(1):101–106.
43. Na M, Ding Y, Wang B, et al. Anti-infective discorhabdins from a deep-water Alaskan sponge of the genus *Latrunculia*. *Indian J Nat Prod Resour*. 2009;73(3):383–387. doi:10.1021/np900281r
44. Cheung RCF, Wong JH, Pan WL, et al. Antifungal and antiviral products of marine organisms. *Appl Microbiol Biotechnol*. 2014;98(8):3475–3494. doi:10.1007/s00253-014-5575-0
45. Hirano K, Kubota T, Tsuda M, Mikami Y, Kobayashi J. Pyrinodems BD, potent cytotoxic bis-pyridine alkaloids from marine sponge *Amphimedon* sp. *Chem Pharm Bull*. 2000;48(7):974–977. doi:10.1248/cpb.48.974
46. Kubota T, Kamijyo Y, Takahashi-Nakaguchi A, Fromont J, Gonoï T, Kobayashi J. Zamamiphidin A, a new manzamine related alkaloid from an Okinawan marine sponge *Amphimedon* sp. *Org Lett*. 2013;15(3):610–612. doi:10.1021/ol3034274
47. Sakurada T, Gill MB, Frausto S, et al. Novel N-methylated 8-oxoisoguanines from Pacific sponges with diverse neuroactivities. *Eur J Med Chem*. 2010;53(16):6089–6099. doi:10.1021/jm100490m
48. Ovenden SP, Capon RJ, Lacey E, Gill JH, Friedel T, Wadsworth D. Amphilactams A–D: novel nematocides from Southern Australian Marine sponges of the Genus *Amphimedon*. *JOC*. 1999;64(4):1140–1144. doi:10.1021/jo981377e
49. Emura C, Higuchi R, Miyamoto T, Van Soest RW. Amphimelibiosides A–F, six new ceramide dihexosides isolated from a Japanese Marine Sponge *Amphimedon* sp. *JOC*. 2005;70(8):3031–3038. doi:10.1021/jo048635u
50. Nemoto T, Yoshino G, Ojika M, Sakagami Y. Amphimic acids and related long-chain fatty acids as DNA topoisomerase I inhibitors from an Australian sponge, *Amphimedon* sp.: isolation, structure, synthesis, and biological evaluation. *Tetrahedron*. 1997;53(49):16699–16710. doi:10.1016/S0040-4020(97)10099-0

51. Shady NH, Fouad MA, Salah Kamel M, Schirmeister T, Abdelmohsen UR. Natural product repertoire of the Genus Amphimedon. *Mar Drugs*. 2018;17(1):19. doi:10.3390/md17010019
52. O'Rourke A. *Bioprospecting of Red Sea Sponges for Novel Antiviral Pharmacophores*. 2015.
53. Costa FG, BRdS N, Gonçalves RL, et al. Alkaloids as Inhibitors of malate synthase from span class="named-content genus-species" id="named-content-1"paracoccidioides span spp.: receptor-ligand interaction-based virtual screening and molecular docking studies, antifungal activity, and the adhesion process. *Antimicrob Agents Chemother*. 2015;59(9):5581–5594. doi:10.1128/AAC.04711-14
54. Montefiori DC. Evaluating neutralizing antibodies against HIV, SIV, and SHIV in luciferase reporter gene assays. *Curr Protoc Immunol*. 2004;64(1):12.11.11–12.11.17. doi:10.1002/0471142735.im1211s64
55. Inc. CCG. *Molecular Operating Environment (MOE)*, 2012.10. 1010 Sherbrooke St.west, Suite #910. Montr. QC, Canada, H3A 2R7; 2012.
56. Nasr T, Bondock S, Eid S. Design, synthesis, antimicrobial evaluation and molecular docking studies of some new thiophene, pyrazole and pyridone derivatives bearing sulfoxazole moiety. *Eur J Med Chem*. 2014;84:491–504. doi:10.1016/j.ejmech.2014.07.052
57. Avilala J, Golla N. Antibacterial and antiviral properties of silver nanoparticles synthesized by marine actinomycetes. *Int J Pharm Sci & Res*. 2019;10(3):1223–1228.
58. Tsuda M, Inaba K, Kawasaki N, Honma K, Kobayashi J. Chiral resolution of (±)-keramaphidin B and isolation of manzamine L, a new β-carboline alkaloid from a sponge Amphimedon sp. *Tetrahedron*. 1996;52(7):2319–2324. doi:10.1016/0040-4020(95)01057-2
59. Tsuda M, Watanabe D, Kobayashi J. Ma'eganedin A, a new manzamine alkaloid from Amphimedon sponge. *Tetrahedron Lett*. 1998;39(10):1207–1210. doi:10.1016/S0040-4039(97)10842-5
60. Kobayashi J, Watanabe D, Kawasaki N, Tsuda M, Nakadomarin A, a novel hexacyclic manzamine-related alkaloid from Amphimedon sponge. *JOC*. 1997;62(26):9236–9239. doi:10.1021/jo9715377
61. Jeong S-J, Inagaki M, Higuchi R, et al. 1, 3-Dimethylisoguaninium, an antiangiogenic purine analog from the sponge amphimedon paraviridis. *Chem Pharm Bull*. 2003;51(6):731–733. doi:10.1248/cpb.51.731
62. Tsukamoto S, Takahashi M, Matsunaga S, Fusetani N, Van Soest RW. Hachijodines A–G: seven new cytotoxic 3-alkylpyridine alkaloids from two marine sponges of the Genera Xestospongia and Amphimedon. *J Nat Prod*. 2000;63(5):682–684. doi:10.1021/np9905766
63. Nishi T, Kubota T, Fromont J, Sasaki T, Kobayashi J. Nakinadines B–F: new pyridine alkaloids with a β-amino acid moiety from sponge Amphimedon sp. *Tetrahedron*. 2008;64(14):3127–3132. doi:10.1016/j.tet.2008.01.111
64. Tsuda M, Kawasaki N, Kobayashi J. Ircinols A and B, first antipodes of manzamine-related alkaloids from an Okinawan marine sponge. *Tetrahedron*. 1994;50(27):7957–7960. doi:10.1016/S0040-4020(01)85280-7
65. Kobayashi J, Tsuda M, Kawasaki N, Sasaki T, Mikami Y. 6-Hydroxymanzamine A and 3, 4-dihydranzamine A, new alkaloids from the Okinawan marine sponge Amphimedon Sp. *J Nat Prod*. 1994;57(12):1737–1740. doi:10.1021/np50114a021
66. Watanabe D, Tsuda M, Kobayashi J. Three new manzamine congeners from amphimedon sponge. *J Nat Prod*. 1998;61(5):689–692. doi:10.1021/np970564p
67. Carballeira NM, Restituyo J. Identification of the new 11, 15-icosadienoic acid and related acids in the sponge Amphimedon complanata. *J Nat Prod*. 1991;54(1):315–317. doi:10.1021/np50073a043
68. Carballeira NM, Colón R, Emiliano A. Identification of 2-methoxyhexadecanoic acid in Amphimedon compressa. *J Nat Prod*. 1998;61(5):675–676. doi:10.1021/np970578v
69. Carballeira NM, Negrón V, Reyes ED. Novel monounsaturated fatty acids from the sponges Amphimedon compressa and Mycale laevis. *J Nat Prod*. 1992;55(3):333–339. doi:10.1021/np50081a009
70. Takekawa Y, Matsunaga S, van Soest RW, Fusetani N. Amphimedosides, 3-alkylpyridine glycosides from a marine sponge Amphimedon sp. *J Nat Prod*. 2006;69(10):1503–1505. doi:10.1021/np060122q
71. Kobayashi J, Tsuda M, Kawasaki N, Matsumoto K, Adachi T. Keramaphidin B, a novel pentacyclic alkaloid from a marine sponge Amphimedon sp.: a plausible biogenetic precursor of manzamine alkaloids. *Tetrahedron Lett*. 1994;35(25):4383–4386. doi:10.1016/S0040-4039(00)73362-4
72. Schmitz FJ, Agarwal SK, Gunasekera SP, Schmidt PG, Shoolery JN. Amphimedine, new aromatic alkaloid from a pacific sponge, Amphimedon sp. carbon connectivity determination from natural abundance carbon-13-carbon-13 coupling constants. *J Am Chem Soc*. 1983;105(14):4835–4836. doi:10.1021/ja00352a052
73. Beran RK, Serebrov V, Pyle AM. The serine protease domain of hepatitis C viral NS3 activates RNA helicase activity by promoting the binding of RNA substrate. *J Biol Chem*. 2007;282(48):34913–34920. doi:10.1074/jbc.M707165200
74. Beran RK, Pyle AM. Hepatitis C viral NS3-4A protease activity is enhanced by the NS3 helicase. *J Biol Chem*. 2008;283(44):29929–29937. doi:10.1074/jbc.M804065200
75. Morgenstern KA, Landro JA, Hsiao K, et al. Polynucleotide modulation of the protease, nucleoside triphosphatase, and helicase activities of a hepatitis C virus NS3-NS4A complex isolated from transfected COS cells. *J Virol*. 1997;71(5):3767–3775. doi:10.1128/JVI.71.5.3767-3775.1997
76. Lipinski CA. Lead-and drug-like compounds: the rule-of-five revolution. *Drug Discov Today Technol*. 2004;1(4):337–341. doi:10.1016/j.ddtec.2004.11.007
77. Ebejer J-P, Charlton MH, Finn PW. Are the physicochemical properties of antibacterial compounds really different from other drugs? *J Cheminform*. 2016;8(1):30. doi:10.1186/s13321-016-0143-5

International Journal of Nanomedicine

Publish your work in this journal

The International Journal of Nanomedicine is an international, peer-reviewed journal focusing on the application of nanotechnology in diagnostics, therapeutics, and drug delivery systems throughout the biomedical field. This journal is indexed on PubMed Central, MedLine, CAS, SciSearch®, Current Contents®/Clinical Medicine,

Submit your manuscript here: <https://www.dovepress.com/international-journal-of-nanomedicine-journal>

Dovepress

Journal Citation Reports/Science Edition, EMBASE, Scopus and the Elsevier Bibliographic databases. The manuscript management system is completely online and includes a very quick and fair peer-review system, which is all easy to use. Visit <http://www.dovepress.com/testimonials.php> to read real quotes from published authors.